Fabrication and characteristics of nitrogen-doped nanocrystalline diamond/p-type silicon heterojunction

D. Lu, H. D. Li*, S. H. Cheng, J. J. Yuan and X. Y. Lv

Nitrogen-doped nanocrystalline diamond films (N-NDFs) have been deposited on p-type silicon (Si) by microwave plasma chemical vapor deposition. The reaction gases are methane, hydrogen, and nitrogen without the conventional argon (Ar). The N-NDFs were characterized by X-ray diffraction, Raman spectroscopy, and scanning electron microscopy. The grain sizes are of 8~10 nm in dimension. The N-NDF shows n-type behavior and the corresponding N-NDF/p-Si heterojunction diodes are realized with a high rectification ratio of 10^2 at ~ 7.8 V, and the current density reaches to 1.35 A/cm^2 at forward voltage of 8.5 V. The findings suggest that fabricated by CH$_4$/H$_2$/N$_2$ without Ar, the N-NDFs and the related rectifying diodes are favorable for achieving high performance diamond-based optoelectronic devices.

Diamond is an important semiconductor for high-power and high-temperature electronic devices because of its large band gap (5.47 eV) and high thermal conductivity (20 W/cm·K). The realizations of p-type and n-type diamonds by chemical vapor deposition (CVD) are desirable for the applications of diamond-based electronic devices. A p-type diamond can be easily achieved by introducing boron dopant [1], while it is difficult to obtain effective n-type diamond due to the formation of deep donor levels with a large activation energy (e.g., 1.7 eV for nitrogen (N$_2$) doping in bulk diamond [2]) or low doping efficiency (e.g., the compensation ratio reaches to as high as around 50~90% in the phosphorus-doped (001) diamond [3]). Recently, CVD nanocrystalline diamond films (NDFs) have been paid more attentions due to their facile doping, high density of grain boundaries, increased sp^2-carbon bonded content and smooth surface, which lead to numerous optoelectronic and mechanical applications [4]. It was reported that n-type conductivity has been easily realized in the N-NDFs, since the N-atoms present predominantly in grain boundaries and introduce new electronic states associated with carbon π bonds and dangling bonds in the fundamental band gap [5]. The N-NDFs were generally prepared by introducing nitrogen (N$_2$) in the Ar/CH$_4$/H$_2$ [6] or Ar/CH$_4$ [7] source gases. In these cases, N$_2$ is proposed as the n-type dopant, and Ar is favorable for generating more C$_2$ radical precursors to increase the nucleation density and consequently decrease the grain size to nanometer scale. In fact, N-NDFs can also be deposited by CVD without introducing Ar in reaction ambient [9]. There are two advantages for the fabrication process without Ar, on the one hand, the experimental conditions are simplified; on the other hand, the possible negative effects of Ar ions on the devices would be reduced. It is therefore desirable to further investigate the properties of NDFs prepared by H$_2$/CH$_4$/N$_2$ and the corresponding applications in optoelectronic devices.

In this paper, we report the growth of N-NDFs by microwave plasma CVD (MPCVD) with the reaction gases of H$_2$/CH$_4$/N$_2$. The products consist of diamond-phase-rich grains with an average size of ~8 nm. Deposited on p-type silicon (Si), the N-NDF/p-Si heterojunction diodes are realized showing the typical rectifying behavior. The devices have high rectification ratio and large forward current density with a low reverse leakage current.

The N-NDFs were grown by MPCVD system (with AsTeX-1500, 2.45 GHz) using the gas mixture of H$_2$/CH$_4$/N$_2$

State Key Laboratory of Superhard Materials, Jilin University, Changchun 130012, PR China

*Corresponding author. Email: hdli@jlu.edu.cn (H. D. Li). Tel./Fax: +86-431-85168095

with the flow rate ratio of 110/10/30 in sccm. The p-type (111) Si (conductivity: 0.05~0.1 $\Omega^{-1} \cdot cm^{-1}$) substrate was first mechanically abraded with 0.2 μm diamond powders for 10 min, and then was ultrasonically seeded for 30 min in diamond slurry consisting of nano/micro-diamond powders to enhance the nucleation density. Finally, the substrate was cleaned ultrasonically in alcohol and acetone for 5 min. In the deposition process, the applied microwave power and total reaction gas pressure was 250 W and 6.7 kPa. The substrate temperature was kept at about 900°C measured by a two-color infrared ratio thermometer (CHINO, Mode IR-GZ201N). The deposition time was 4 h.

The structure and morphology of the as-synthesized N-NDFs were characterized by means of Raman spectroscopy (Renishaw inVia, excitation wavelength of 514.5 nm), X-ray diffraction (XRD, Rigaku D/max-rA with Cu Kα radiation) and scanning electron microscopy (SEM, JSM-6700F). Optical emission spectroscopy (OES, by Ocean Optics USB4000) was used to measure the species in the $CH_4/H_2/N_2$ plasma. For the electrical measurements of the devices, the silver (Ag) slurry was used as the contacts on the surface of N-NDFs and backside of p-type Si. In order to achieve ohmic contact, the devices were subjected to thermal annealing process at 150°C for 15 min in air. The current voltage (I–V) curves were measured using Keithley sourcemeter 2400 by the two-point probe method. All the examinations were performed at room temperature.

Figure 1(a) shows the SEM image of the N-NDF. The film consists of nanosized grains, which is similar to that deposited in Ar-rich $H_2/CH_4/N_2$ ambient [6,7,10]. Observed from the high magnification image (the inset of Fig. 1), the grains are of 8~10 nm in dimension, and the major grains are aggregated. The surface of the film is relatively loose. The thickness of the
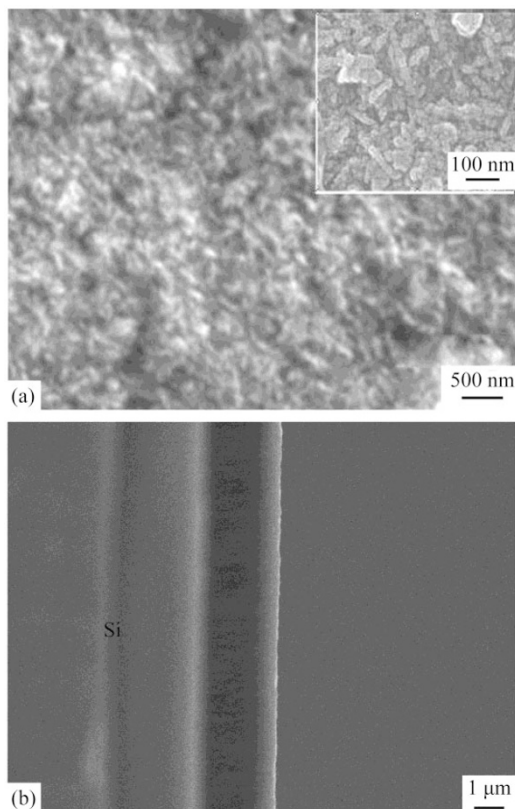

FIG. 1. (a) SEM image of the N-NDF and the inset is the high magnification image, (b) the cross-section SEM image of the N-NDF.

as-grown N-NDF is about 2.8 μm, estimated from the cross-section SEM image shown in Fig. 1(b), and the growth rate is estimated to be about 0.7 μm/h. The OES spectra with different N_2 flow rate are shown in Fig. 2. In the $H_2/CH_4/N_2$ plasma, the CN violet emission (at 387.4 nm and 418.9 nm), hydrogen emission (Hα at 656.5 nm, Hβ at 486 nm) and C_2 Swan band (at 516.2 nm) are observed [11]. Compared with Ar-rich plasma [12] that the C_2 dimers are dominant, the CN species show the strongest intensity in the $CH_4/H_2/N_2$ plasma and the C_2 dimers intensity is very low. As the N_2 flow rate increased from 10 sccm to 30 sccm, the relative intensity of CN/Hα enhanced. Although the CN species do not lead to diamond growth by themselves, the large amount of CN species will be favorable for the formation of more defects and result in the decrease of grain
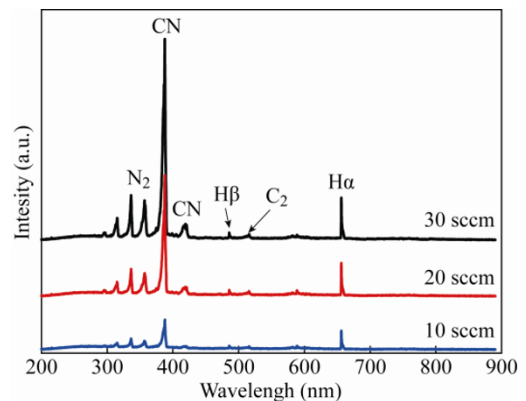

FIG. 2. OES spectra of the $CH_4/H_2/N_2$ plasma with N_2 flow rate from 10 sccm to 30 sccm.

size in NDFs [13].

The typical XRD pattern of the N-NDF is shown in Fig. 3(a). The peaks at 43.9° and 75.6° are assigned to diamond (111) and (220) diffractions, respectively. The average grain size (d) is obtained by Sherer's formula [14]: d=0.9 λ/Bcosθ, where λ = 1.54016 Å and B is the full width at half maximum (FWHM) of the diffraction peak. The average crystal size calculated from (111) peak is about 8.6 nm, which is in consistence with the size observed in SEM image (see Fig. 1).

Figure 3(b) shows the Raman spectrum of the sample. The peak at 1333 cm^{-1} is assigned to the intrinsic zone-centre phonon band of diamond. The broad bands centered at about 1360 cm^{-1} and 1555 cm^{-1} are attributed to the disordered D band and graphitic G band especially related to nanocrystalline diamond (NCD), respectively [6,15,16]. The nitrogen presence in the lattices of N-NCD is demonstrated by the blue shift of 1360 cm^{-1} band from the D band (1340 cm^{-1}) of undoped NCD [15]. Note that there is a shoulder band appearing at about 1150 cm^{-1}, though its origination is still debated. It was previously proposed as a characteristic Raman spectral feature for NCD [17-19]. However, some researchers [15,20] pointed out that the peak should not be attributed to the presence of NCD and/or other sp3-bonded phases, but to trans-polyacetylene segments existing in the grain boundaries. Nevertheless, combined with the above XRD and SEM results, the synthesized products consist mainly of nanosized diamond crystals.

Figure 4(a) and 4(b) show the I-V characteristics of Ag contacts on p-typed Si and N-NDF, respectively. It is found that the observed I-V behaviors are linear for both forward and reverse bias, suggesting that ohmic contacts have been formed
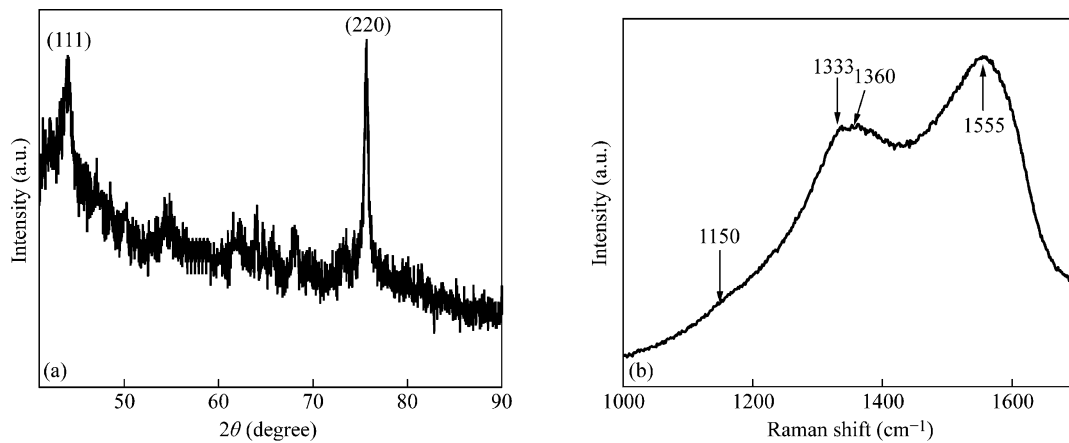
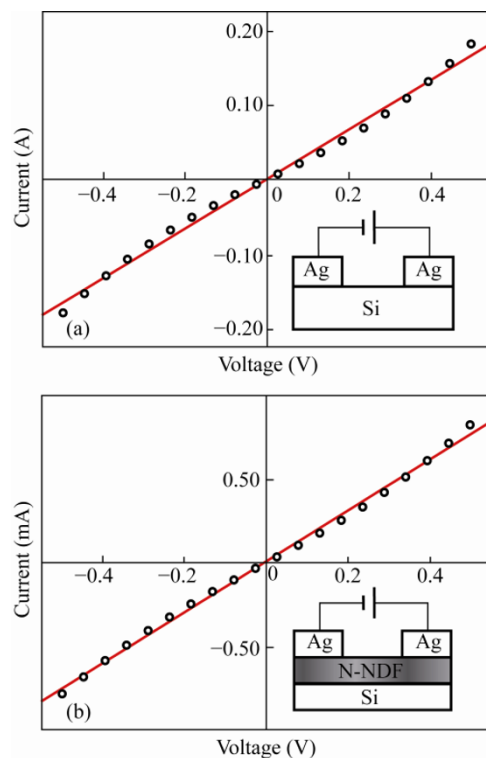FIG. 3. (a) XRD pattern and (b) Raman spectrum of the N-NDF.

FIG. 4. *I-V* characteristics for the interface of (a) Ag/p-type Si and (b) Ag/n-type NDF.

FIG. 5. *I-V* characteristic of the n-NDF/p-Si heterojunction diode.

between Ag/Si and Ag/N-NDF. Note that the current intensity of Ag/Si is about 200 times higher than Ag/N-NDF, indicating that the N-NDF possesses higher resistivity with respect to Si. The resistivity of as-deposited N-NDF is about 10^5 Ω·cm, calculated by the following equation [9]

$$\rho_D = (R - \rho_S L_S / A) A / L_D$$

where R is the total resistance (silicon substrate and NDF) obtained from I-V measurement (~10^3 Ω·cm), A is the area of the electrode (~5 mm^2), ρ_S is the resistivity of silicon substrate (10 Ω·cm), and L_S and L_D are the thickness of silicon substrate (500 μm) and NDF (~2.8 μm) measured from the SEM cross-sectional images, respectively.

The typical current-voltage curve of the N-NDF/p-Si heterojunction diode is shown in Fig. 5. The rectification characteristic is represented with rectification ratios up to 10^2 orders of magnitude at ~7.8 V. The rectifying result suggests that
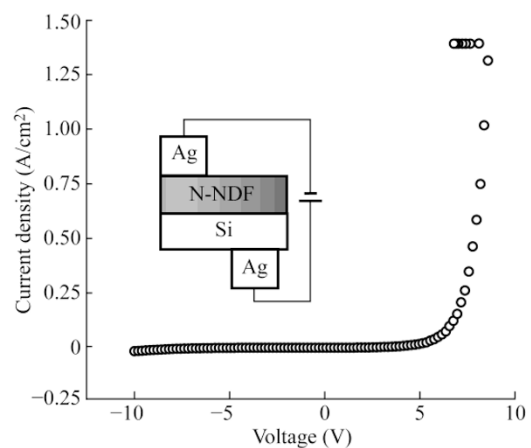
the major carriers for the N-NDF are electrons, i.e., the N-NDF might show n-type characteristic. The turn-on voltage of the heterojunction is about 4.8 V, and the current density can achieve to 1.35 A/cm^2 at a forward bias of 8.5 V. These data are comparable with that obtained from the case of N-NDF fabricated in the system of Ar/CH$_4$/N$_2$ [8]. Moreover, when the reverse-bias increases as high as ~10 V, the leakage current is small (~0.015 A/cm^2), which can be related to the low conductivity (<10^{-5} Ω^{-1}·cm^{-1}) of the N-NDF measured by the Van der Pauw method. The high resistivity is proposed to be attributed to the loose feature represented in the N-NDF (see Fig. 1). In addition, for the NDFs grown in the H$_2$-rich plasma of CH$_4$/H$_2$/N$_2$, the hydrogen atoms can easily bind with the unpaired electrons of the doped nitrogen atoms, resulting in a lower electrical conductivity [21]. Interestingly, it is found that no saturation trend appears for the forward current at ~9 V, implying that the current can reach higher value with the increase of forward voltage, leading to higher rectification ratio. Due to the current limit of the test equipment, the experiments performed at high forward voltages (>10 V) were not carried out.

Ma [9,13] mentioned that the increasing concentration of CN species may be the reason for the formation of ordered sp^2-bond carbon and thus decrease the film resistivity from 10^9 to 10^5 Ω·cm which is still higher than the Ar- rich plasma prepared films. In the NDFs deposited by CH$_4$/H$_2$/N$_2$ plasma, the adding of N$_2$ introduces few new electronic states in the band gap. However, new states exist in the NDFs prepared by Ar- rich plasma through the theoretical prediction [5,22]. Due to less

mid-gap states in our N-NDF, the interfacial barrier potential in the NDF/Si interface is higher than samples of the Ar-rich plasma [8]. The high interfacial barrier potential may be the main reason for the high turn-on voltage (~4.8 V). Meanwhile, the less new defect states near the Fermi level regarded as leakage current source [8] in our specimen is beneficial for achieving a comparatively small leakage current (~0.015 A/cm^2 at 10 V) in the N-NDF/p-Si heterojunction.

In summary, the growth and characterization of the N-NDF deposited by MWCVD in $N_2/CH_4/H_2$ are reported. The N-NDF/p-Si heterojunction diodes have been achieved having high rectification ratio of 10^2 and high current density (1.35 A/cm^2 at forward bias of 8.5 V) with low leakage reverse current. It is demonstrated that the N-NDFs fabricated without the conventional Ar can also be used to realize high performance diamond-based optoelectronic devices.

References

1. R. Kalish, Carbon 37, 781 (1999). doi:10.1016/S0008-6223(98)00270-X.
2. P. K. Sitch, G. Jungnickel, M. Kaukonen, D. Porezag, Th. Frauenheim, M. R. Pederson and K. A. Jackson, J. Appl. Phys. 83, 9 (1998). doi:10.1063/1.367249
3. H. Kato, S.Yamasaki and H. Okushi, Diamond Relat. Mater. 16, 796 (2007). doi:10.1016/j.diamond.2006.11.085
4. K. Subramanian, W. P. Kang and J. L. Davidson, Proceeding 18th IVNC, 198 (2005).
5. P. Zapol, M. Sternberg, L. A. Curtiss, T. Frauenheim and D. M. Gruen, Phys. Rev. B 65, 045403 (2001). doi:10.1103/PhysRevB.65.045403
6. Q. Hu, M. Hirai, R. K. Joshi and A. Kumar, J. Phys. D: Appl. Phys. 42, 025301 (2009).
7. S. Bhattacharyya, O. Auciello, J. Birrell, J. A. Carlisle, L.A. Curtiss, A. N. Goyette, D. M. Gruen, A.R. Krauss, J. Schlueter, A. Sumant and P. Zapol, Appl. Phys. Lett. 79, 1441 (2001). doi:10.1063/1.1400761
8. T. Ikeda and K. Teii, Appl. Phys. Lett. 94, 072104 (2009). doi:10.1063/1.3082045
9. K. L. Ma, W. J. Zhang, Y. S. Zou, Y. M. Chong, K. M. Leung, I. Bello and S.T. Lee, Diamond Relat. Mater. 15, 626 (2006). doi:10.1016/j.diamond.2005.11.017
10. T. D. Corrigan, D. M. Gruen, A. R. Krauss, P. Zapol and R. P. H. Chang, Diamond Relat. Mater. 11, 43 (2002). doi:10.1016/S0925-9635(01)00517-9
11. T. Vandevelde, M. Nesladek, C. Quaeyhaegens and L. Stals, Thin Solid Films 290, 143 (1999). doi:10.1016/S0040-6090(96)09189-4
12. Y. K. Liu, P. L. Tso, D. Pradhan, I. N. Lin, M. Clark and Y. Tzeng, Diamond Relat. Mater. 14, 2059 (2005). doi:10.1016/j.diamond.2005.06.012
13. K. L. Ma, J. X. Tang, Y. S. Zou, Q. Ye, W. J. Zhang and S. T. Lee, Appl. Phys. Lett. 90, 092105 (2007). doi:10.1063/1.2709953
14. B. D. Cullity, Elements of X-Ray Diffraction (Addison-Wesley, Reading,MA, 1978).
15. A. C. Ferrari and J. Robertson, Phys. Rev. B 63, 121405 (2001). doi:10.1103/PhysRevB.63.121405
16. J. Birrell, J. E. Gerbi, O, Auciello, J. M. Gibson, D. M Gruen and L.A. Carlisle, J. Appl. Phys. 93, 5606 (2003). doi:10.1063/1.1564880
17. W. A. Yarbrough and R. Messier, Science 247, 688 (1990). doi:10.1126/science.247.4943.688
18. J. Nemanich, J. T. Glass, G. Lucovsky and R. E. Shroder, J. Vac. Sci. Technol. A 6, 1783 (1988). doi:10.1116/1.575297
19. R. E. Shroder, R. J. Nemanich and J. T. Glass, Phys. Rev. B 41, 3738 (1990). doi:10.1103/PhysRevB.41.3738
20. R. Pfeiffer, H. Kuzmany, P. Knoll, S. Bokova, N. Salk and B. Gunther, Diamond Relat. Mater. 12, 268 (2003). doi:10.1016/S0925-9635(02)00336-9
21. S. Raina, W. P. Kang, J. L. Davidson and X. C. LeQuan, 215th ECS Meeting (2009).
22. P. Achatz, O. A. Williams, P. Bruno, D. M. Gruen, J. A. Garrido and M. Stutzmann, Phys. Rev. B 74, 155429 (2006). doi:10.1103/PhysRevB.74.155429